THE NEWTONIAN AND MOND DYNAMICAL MODELS OF NGC 5128: INVESTIGATION OF THE DARK MATTER CONTRIBUTION

S. Samurović

Astronomical Observatory, Volgina 7, 11060 Belgrade 74, Serbia

E–mail: *srdjan@aob.rs*

SUMMARY: We study the well-known nearby early-type galaxy NGC 5128 (Centaurus A) and use the sample of its globular clusters to analyze its dynamics. We study both Newtonian and MOND models assuming three cases of orbital anisotropies: the isotropic case, mildly tangentially anisotropic case and the radially anisotropic case based on the literature. We find that there are two regions with different values of the velocity dispersion: the interior up to ~ 3 effective radii where the velocity dispersion is approximately 150 $\mathrm{km\,s^{-1}}$, whereas beyond ~ 3 effective radii its value increases to approximately 190 $\mathrm{km\,s^{-1}}$, thus implying the increase of the total cumulative mass which is indicative of the existence of dark matter there in the Newtonian approach: the mass-to-light increases from $M/L_B = 7$ in the inner regions to $M/L_B = 26$ in the outer regions. We found that the Navarro-Frenk-White (NFW) model with dark halo provides a good description of the dynamics of NGC 5128. Using three MOND models (standard, simple and toy), we find that they all provide good fits to the velocity dispersion of NGC 5128 and that no additional dark component is needed in MOND.

Key words. galaxies: kinematics and dynamics — galaxies: elliptical, and lenticular — galaxies: structure – dark matter — galaxies: individual: NGC5128

1. INTRODUCTION

Although significant efforts have been made, the solution to the dark matter (DM) problem still eludes us. Since this is the problem which emerged mainly from the dynamics of spiral galaxies it is not strange that spirals (late-type galaxies) were best studied using their rotation curves as the tracers of the total dynamical mass (see, e.g. Binney and Tremaine 2008). On the other hand, early-type galaxies (hereafter ETGs, elliptical and lenticular galaxies) contain little or no cool gas and the usage of 21-cm observations to trace kinematics of neutral hydrogen out to large radii is not feasible and other methodologies have to be used to accurately establish the total dynamical mass out to large radii. These outer regions of ETGs are especially important because one expects that DM dominates the luminous matter there. Various techniques to study DM in ETGs are presented in Samurović (2007) and here we will provide briefly only basic information.

Since in the present paper we deal with both Newtonian and MOND (Modified Newtonian Dynamics) approaches we here briefly note the advantages and disadvantages of both approaches. For Newtonian models (see, e.g. Bertin 2014), it is well known that they provide good fits for the observed kinematics of both spirals and ellipticals, and the main drawback is that their main ingredient, the hypothetical DM particle has not been identified yet after long and detailed searches. On the other hand,

MOND based on the theoretical modification of the Newtonian theory, is expected to provide successful fits for observed galaxies without DM. One of the biggest successes of MOND is no doubt its ability to fit spiral galaxies without DM (for a review, see e.g. Sanders and McGaugh 2002). However, when ETGs are modeled using MOND, the results are mixed and the existence of additional, dark, component cannot be excluded in numerous cases (see below, for more details). Also, it is well known that MOND has problems at the scales of clusters of galaxies (see, e.g. Sanders 2003) where additional dark mass appears to be necessary. The well-known case of the Bullet Cluster (1E 0657-558) which consists of two colliding clusters of galaxies, was considered as the best example in favor of DM (Bradač et al. 2006). Recently, MOND was also used in various numerical simulations: see, e.g. the work of Angus et al. (2014) where the cosmological particle-mesh N-body code was used to investigate the feasibility of structure formation in a framework involving MOND and light sterile neutrinos, which means that an additional, hypothetical dark particle is needed. It is worth noting that an another interesting line of investigation of MOND is that based on the study of shell galaxies and promising results have been obtained (Bílek et al. 2015) which may lead to further tests of the DM/MOND dichotomy in the future. Therefore, as will be shown below, since the number of early-type galaxies studied using MOND is still small, it is important to study as many interesting objects as possible, and NGC 5128 being the nearest large elliptical galaxy is certainly worth investigating.

Although the studies of *stellar kinematics* were until recently restricted to the inner parts of ETGs of a small number of objects (see, e.g. Samurović and Danziger 2005), the situation is now changing favorably because new surveys provide information on dynamics out to larger radial distances for larger samples: e.g. Foster et al. (2015) published recently their results of the SLUGGS (SAGES Legacy Unifying Galaxies and GlobularS)[1] study od 25 ETGs and presented kinematic maps out to 2.6 effective radii (one effective radius, R_e, is the radius of the isophote containing half the total luminosity of a given galaxy) on average. The studies of ETGs that use *X-rays* as a tracer of their mass are important because such studies do not suffer from the so-called mass-anisotropy degeneracy that introduces significant uncertainty in dynamical analyzes based on other tracers. This degeneracy leads to the problem of determination of the mass in ETGs and is due to the fact that one does not *a priori* know anything about the orbits of stars in ellipticals (see Tonry 1983, see also Binney and Merrifield 1998, Chap 11.2). X-ray studies strongly suggest the rise of the total dynamical mass in ETGs thus implying significant amounts of DM in their outer parts.

Planetary nebulae (PNe) are widely used in DM research because they are detectable even in moderately distant galaxies through their strong emission lines. The usage of PNe in the case of ETGs led to various conclusions: e.g. Romanowsky et al. (2003) observed PNe in three galaxies (NGC 821, NGC 3379 and NGC 4494) and found little or no dark matter out to $\sim 3.5\ R_e$; the conclusion was later modified in the paper of De Lorenzi et al. (2009) in which it is claimed that "NGC 3379 may well have a DM halo as predicted by recent merger models within ΛCDM cosmology, provided its outer envelope is strongly radially anisotropic". *Globular clusters (GCs)* are a very promising tool in the study of DM in ETGs. The work of Deason et al. (2012) summarizes the results found in the literature for 15 elliptical galaxies for observations based on PNe and GCs. Samurović (2014, hereafter S14) used a sample of 10 ETGs coming from the SLUGGS sample of Pota et al. (2013) as tracers of the gravitational potential of the galaxies in a sample in both the Newtonian (mass-follows-light and dark matter models) and the MOND approaches and found that Newtonian mass-follows-light models without a significant amount of dark matter can provide successful fits for only one galaxy (NGC 2768) whereas the remaining nine ETGs require various amounts of DM in their outer parts (beyond $2-3R_e$); Samurović also found that MOND alone is not sufficient to fully explain the dynamics of six galaxies in the sample. *Gravitation lensing* is also used in the investigation of DM in ETGs: e.g. Kleinheinrich et al. (2006) used weak lensing studies to analyze singular isothermal spheres and Navarro-Frenk-White (Navarro et al. 1997, hereafter NFW) profiles for a sample of lenses at redshift $z = 0.2 - 0.7$ and found that ETGs have 2-3 times more massive halos than their late-type counterparts at the same luminosity. Also, the surveys dedicated to the study of strong lensing were used for providing the information required to compare ETGs at intermediate redshifts to nearby objects: e.g. Tortora et al. (2010) analyzed the correlations among central DM content of ETGs, their sizes, and their ages, using a sample of gravitational lenses from the SLACS (Sloan Lens ACS Survey)[2] at $z \sim 0.2$, and compared them with a larger sample of $z \sim 0$ galaxies and found that their results agree with studies based on local galaxies.

The investigation of DM in ETGs based on various tracers thus led to different conclusions regarding their inner (interior to $\sim 1-3R_e$) and outer (exterior to $\sim 1-3R_e$) parts: in most of the studied cases, DM does not dominate in the inner regions, whereas in the outer regions DM may or may not dominate. Also, for some ETGs MOND can provide satisfactory description of their dynamics, and for some others, MOND is insufficient and additional DM is needed in their outer parts.

---

[1] http://sluggs.swin.edu.au

[2] http://www.slacs.org

The nearby ETG NGC 5128 remains an interesting object for various types of studies for its proximity and the availability of various observations made using different techniques. In this paper we updated our previous results presented in Samurović (2006) related to the study of GCs in this galaxy and we also make a comparison with the results from our paper based on PNe in NGC 5128 (Samurović 2010). Also, we place NGC 5128 in the context of other recently analyzed ETGs (S14) in both frameworks, the Newtonian and MOND.

The example of the galaxy NGC 5128 is an interesting one because different observations based on different techniques are available making thus possible a thorough comparison out to large distance from the center (out to $\sim 8R_{\rm e}$).

The plan of this paper is as follows: In Section 2 we present the basic observational data related to NGC 5128 concerning photometry and GCs and the results concerning their kinematics. In Section 3 we describe the theoretical aspects of the Jeans analysis of the dynamics and use the Jeans equation in both Newtonian and MOND approach to determine the best-fit parameters for our dynamical models. In Section 4 we discuss our findings and finally, in Section 5 we present the conclusions.

## 2. OBSERVATIONAL DATA AND KINEMATICS OF NGC 5128

2.1. NGC 5128 (Cen A)

NGC 5128 (also known as the radio source Centaurus A) is the nearest large elliptical galaxy and in this paper we use the distance $D = 3.84 \pm 0.35$ Mpc from Rejkuba (2004). At this distance $1' \approx 1.12$ kpc meaning that $1'' \approx 18.62$ pc. The effective radius is $R_{\rm e} = 305$ arcsec (Dufour et al. 1979) and the systemic velocity is $v_{\rm syst} = 541$ km s^{-1}. The B–band luminosity of the stellar component NGC 5128 is $L_B = 3.98 \times 10^{10} L_{\odot}$. We refer the reader to the complete review of this galaxy available in the paper by Israel (1998).

2.2. Globular clusters of NGC 5128

In the present paper we use the sample coming from the paper by Woodley et al. (2010) which consists of 530 (263 metal-poor, i.e. blue and 267 metal-rich, i.e. red) GCs that extend out to ~ 45 arcmin. As in Samurović (2006) we worked with a *total* sample of GCs to have more clusters per bin because our goal is to determine as accurately as possible the velocity dispersion and departures from the Gaussian in the distribution of GCs[3]. For completeness, in Table 1 we also include the kinematics of both the blue and red GC population: due to the smaller number of tracers per bin, the errors of all quantities are inevitably larger, but for the bins where the number of tracers is approximately the same for both populations, the red population shows either higher

or approximately same values of the velocity dispersion with respect to their blue counterparts. For the volume density slope of the total sample of GCs, we used in the Jeans equation (see below) the value calculated by Woodley et al. (2010), $\alpha = 3.38$ (see their Fig. 9). For the rotation of the GCs in our sample we used the value $v_{\rm rot} = 33$ km s^{-1} also calculated by Woodley et al. (2010). Throughout the paper, we assume the dimensionless Hubble constant $h_0 = 0.70$.
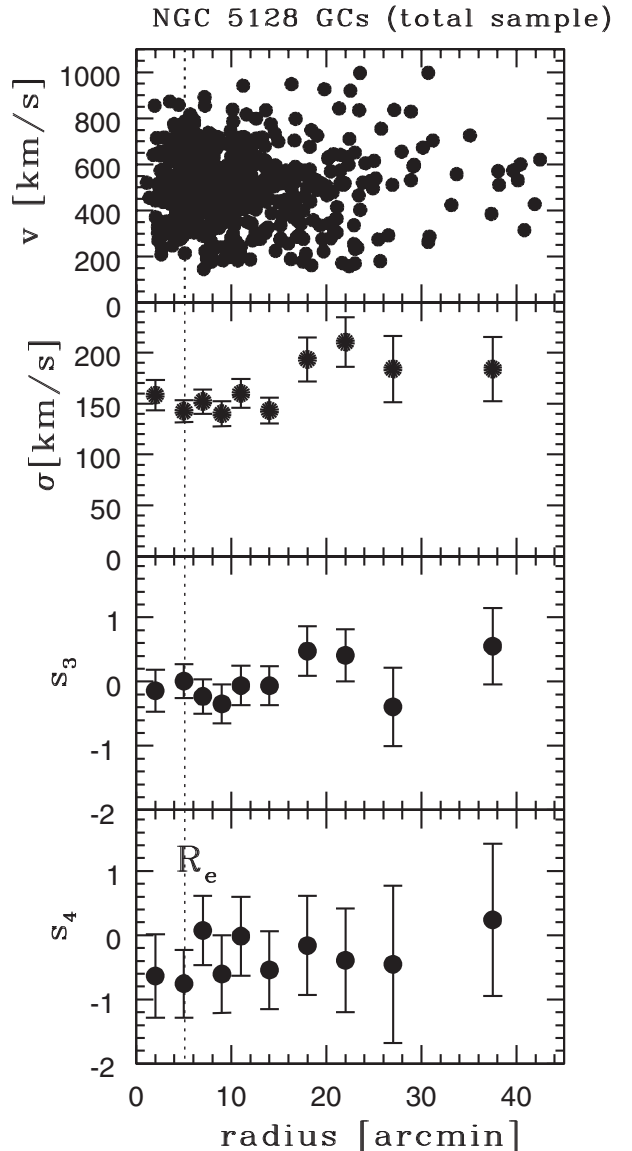
Fig. 1. *Kinematics of GCs belonging to NGC 5128. From top to bottom: radial velocities of the GCs, velocity dispersions, asymmetric (s_3) and symmetric departures (s_4) from Gaussian as function of radius.*

---

[3] As noted in S14, one should bear in mind that red and blue GCs may in principle have different kinematics and their velocity anisotropies may be different.

The kinematics of NGC 5128 based on the GCs is given in Table 1 and also in Fig. 1: from top to bottom we plot function of radius for: the radial velocity, velocity dispersion, the s_3 and s_4 parameters which describe skewness and kurtosis, i.e. asymmetric and symmetric departures from the Gaussian, respectively.

2.3. Determination of kinematics of NGC 5128

In the present paper, we rely on the methodology established in Samurović (2006): we used standard definitions implemented in the NAG (Numerical Algorithms Group) routine G01AAF[4] to calculate the velocity dispersion as well as anisotropies deter-

Table 1. Projected velocity dispersion measurements of GCs in NGC 5128.

r (arcmin) (1)	σ (km s^{-1}) (2)	err_σ (km s^{-1}) (3)	s_3 (4)	err_s_3 (5)	s_4 (6)	err_s_4 (7)	N (8)
Total sample of GCs							
2.0	158	15	-0.14	0.32	-0.63	0.65	57
5.0	143	11	0.01	0.26	-0.76	0.53	86
7.0	152	12	-0.23	0.27	0.07	0.54	82
9.0	140	12	-0.35	0.30	-0.61	0.60	66
11.0	160	14	-0.06	0.31	-0.02	0.61	64
14.0	143	13	-0.07	0.30	-0.54	0.61	65
18.0	194	22	0.48	0.39	-0.16	0.77	40
22.0	210	24	0.41	0.40	-0.39	0.81	37
27.0	184	33	-0.39	0.61	-0.45	1.22	16
37.5	184	32	0.55	0.59	0.24	1.19	17
Blue GCs							
2.0	132	21	-0.11	0.55	-1.06	1.10	20
5.0	146	16	0.10	0.37	-0.54	0.75	43
7.0	151	18	-0.24	0.41	-0.09	0.82	36
9.0	124	15	-0.60	0.43	0.18	0.85	33
11.0	154	18	-0.20	0.41	-0.73	0.83	35
14.0	148	17	-0.06	0.41	-0.69	0.82	36
18.0	187	30	0.72	0.55	0.52	1.09	20
22.0	195	34	0.22	0.59	-1.02	1.19	17
27.0	212	50	-0.19	0.82	-1.29	1.63	9
37.5	156	29	-0.18	0.65	-1.39	1.31	14
Red GCs							
2.0	172	20	-0.22	0.40	-0.70	0.81	37
5.0	138	15	-0.05	0.37	-1.07	0.75	43
7.0	153	16	-0.24	0.36	0.14	0.72	46
9.0	149	18	-0.04	0.43	-0.97	0.85	33
11.0	164	22	0.01	0.45	0.41	0.91	29
14.0	140	18	-0.06	0.45	-0.43	0.91	29
18.0	199	31	0.24	0.55	-0.61	1.10	20
22.0	220	35	0.44	0.55	-0.45	1.10	20
27.0	129	34	0.84	0.93	-1.17	1.85	7
37.5	264	108	0.54	1.41	-2.00	2.83	3

NOTES – Col. (1): radial bin. Col. (2): velocity dispersion. Col. (3): formal errors for the velocity dispersion. Col. (4): the s_3 parameter. Col. (5): formal errors for the s_3 parameter. Col. (6): the s_4 parameter. Col. (7): formal errors for the s_4 parameter. Col. (8): number of GCs in a given bin.

---

mined by the s_3 and s_4 parameters. As can be seen from Table 1 and Fig. 1, the error bars for all the quantities increase in the outer parts because of the smaller number of GCs per bin. The anisotropies are small and, in most cases, consistent with zero, i.e. with isotropic distribution of the objects.

One can see in Table 1 and also in Fig. 1 that the velocity dispersion remains approximately constant ($\sigma \sim 150$ km s^{-1}) inside the interior up to ~ 14 arcmin ($2.8R_\mathrm{e}$) and it rises ($\sigma \gtrsim 190$ km s^{-1}) beyond $\sim 3R_\mathrm{e}$, implying the rising of the total cumulative mass which is indicative of strong contribution of DM there (see the text below for detailed discussion).

3. THE JEANS MODELLING OF NGC 5128

The Jeans modeling performed in the present paper closely follows the approach applied in S14 and the reader is referred to that paper for more information because only the most important information are provided below.

The spherical Jeans equation which provides the connection between the velocity distribution, the anisotropy of the tracers and the total dynamical mass is of the form (Jeans 1915, Duncan and Wheeler 1980, Binney and Tremaine 2008):

$$\frac{\mathrm{d}\sigma_r^2}{\mathrm{d}r} + \sigma_r^2 \frac{(2\beta + \alpha)}{r} = a_\mathrm{N;M} + \frac{v_\mathrm{rot}^2}{r}, \qquad (1)$$

and is valid for both approaches, the Newtonian ("N") and MOND ("M"): $a_\mathrm{N;M}$ is an acceleration term which is different for each approach. In the Newtonian approach it is equal to $a_\mathrm{N} = -\frac{GM(r)}{r^2}$ and for MOND ('M') models $a_\mathrm{M}\mu(a_\mathrm{M}/a_0) = a_\mathrm{N}$ (see below for expressions of function μ). The radial velocity dispersion is designated by σ_r and $\alpha = d\ln\rho/d\ln r$ is the slope of the density of GCs and is always taken to be 3.38 as given above. The rotational component is always taken to be $v_\mathrm{rot} = 33$ km s^{-1} as also indicated above. We note that if we neglect the rotational speed, i.e. when we assume $v_\mathrm{rot} = 0$ km s^{-1}, the total modeled mass-to-light is *increased* by approximately 4 %. On the other hand, if we assume $v_\mathrm{rot} = 100$ km s^{-1} (see, Samurović 2006) the inferred mass-to-light ratio is *decreased* by approximately 16%. Therefore, we may conclude, that the uncertainty of the measurement of the rotational component does not influence much our final results and conclusions.

The anisotropy of the orbits of GCs is expressed using the following expression:

$$\beta = 1 - \frac{\overline{v_\theta^2}}{\sigma_r^2}, \qquad (2)$$

where $\overline{v_\theta^2} = \overline{v_\theta}^2 + \sigma_\theta^2$ and $0 < \beta < 1$ means that the orbits are predominantly radial (equivalent to

$s_4 > 0$), whereas for $-\infty \leq \beta < 0$ the orbits are mostly tangential (equivalent to $s_4 < 0$) (Gerhard 1993).

The projected line-of-sight velocity dispersion is always given as (Binney and Mamon 1982):

$$\sigma_p^2(R) =$$
$$= \frac{\int_R^{r_\mathrm{t}} \sigma_r^2(r)\left[1 - (R/r)^2\beta\right]\rho(r)(r^2 - R^2)^{-1/2}rdr}{\int_R^{r_\mathrm{t}} \rho(r)(r^2 - R^2)^{-1/2}rdr}, (3)$$

where the truncation radius, r_t, extends beyond the observed kinematical point of the highest galactocentric radius.

In all our dynamical models, we deal with three cases of anisotropies:

a) the lack of anisotropy (the isotropic case), as the most general case ($\beta = 0$),

b) the theoretically based case coming from the literature (see Mamon and Łokas 2005), for which:

$$\beta(r) = \beta_0 \frac{r}{(r + r_a)}, \qquad (4)$$

where $\beta_0 \simeq 0.5$ and $r_a \simeq 1.4R_\mathrm{e}$; this estimate which is radially dominated since $\beta > 0$, comes from theoretical expectations from merging collisionless systems; we denote the values of the β parameter thus calculated as β_lit in the text below, and

c) a mildly tangentially dominated case (for which we have a hint from the negative values of the s_4 parameter for the most calculated points, see Fig. 1, the lowest panel) for which $\beta = -0.20$.

The best-fitting results obtained using the Jeans equation are presented in Figs. 2–6 below.

In both approaches we always rely on a Newtonian constant mass-to-light ratio Sérsic model (see S14 for details) that uses field stars of NGC 5128 and for which the Sérsic index $n_* = 4.0$ was used (see below for more details). A certain value of the stellar mass-to-light is assumed, i.e. the contribution of the visible, stellar matter. Additional details relevant to both approaches are described below.

We compare our estimates of the dynamically inferred values of the mass-to-light ratio in various models with the predictions coming from several stellar population synthesis (SPS) models based on the paper by Bell and De Jong (2001). All the models, together with metallicity and initial mass functions (IMFs) used, are given in Table 2. The models are based on the corrected $B - V$ color from the HyperLeda database for NGC 5128: $B - V = 0.87$.

The result of application of the purely constant mass-to-light ratio model is shown in Fig. 2. It is obvious that a model with one fixed mass-to-light ratio cannot describe correctly the dynamics of NGC 5128: in the inner region, interior up to $\sim 3R_\mathrm{e}$, the inferred value of the mass-to-light ratio, $M/L_B = 7.0$ is consistent with the IP13 Salpeter model and the lack of DM there. However, beyond $\sim 3R_\mathrm{e}$ the mass-to-light ratio increases and becomes equal to 26.0, which means that, between ~ 3 and $\sim 8R_\mathrm{e}$, DM dominates and comprises at least 70 per cent of the total mass budget in the Newtonian approximation.

Table 2. Values of the predicted stellar mass-to-blue-light ratios in various theoretical SPS models.

	BC model	PEGASE model	IP13 model1	IP13 model2	IP13 model
IMF metallicity (Z)	Salpeter 0.02	Salpeter 0.02	Kroupa ≤ 0.03	Kroupa ≤ 0.03	Salpeter ≤ 0.03
	(1)	(2)	(3)	(4)	(5)
M/L_*	5.6	6.2	3.5	3.9	6.8

NOTES – Col. (1): the SPS Bruzual and Charlot (Bruzual and Charlot 2003, BC) model with Salpeter IMF for $Z = 0.02$. Col. (2): the SPS PEGASE (Fioc and Rocca-Volmerange 1997) model with Salpeter IMF for $Z = 0.02$. Col. (3): the exponential SFH model with the Kroupa IMF (Into and Portinari 2013, IP13). Col. (4): the disc galaxy model based on the Kroupa IMF (Into and Portinari 2013, IP13). Col. (5): the disc galaxy model based on the Salpeter IMF (Into and Portinari 2013, IP13).
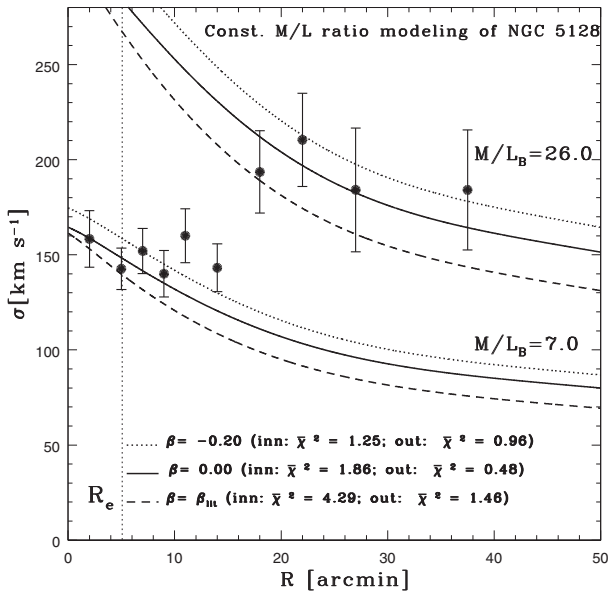
Fig. 2. *Jeans modeling of the GCs of NGC 5128 for the Newtonian mass-follows-light cases. Lower three lines are for the case for which $M/L_B = 7.0$ and the upper three lines are for the case for which $M/L_B = 26.0$. For both values of the mass-to-light ratio, the thin solid line is for the isotropic case ($\beta = 0$), dotted lines are for the case of mildly tangential anisotropies ($\beta = -0.20$) and the dashed lines are for the radially anisotropic theoretical case ($\beta = \beta_{\rm lit}$), see text for details). The vertical dotted line here and in all figures related to the Jeans models below denotes one effective radius of NGC 5128. Here, and in all figures related to the Jeans models below, the reduced $\bar{\chi}^2$ value is given for the each best-fitting value. Only in this particular figure are the $\bar{\chi}^2$ values given for the inner and the outer part.*

3.1. Newtonian DM models

Since the constant mass-follows-light model cannot reproduce the dynamics of NGC 5128, we first apply Newtonian approach with the additional dark component in the form of the NFW DM halo. The NFW density has the following form:

$$\rho(x) = \frac{4\rho_{\rm s}}{x(x+1)^2}, \qquad (5)$$

where $x = r/r_{\rm s}$, $r_{\rm s}$ is the scale radius at which the logarithmic slope of the NFW density profile is -2, while $\rho_{\rm s}$ is the density at that radius. This halo is added to the visible stellar component calculated using the Sérsic model as given above.

The stellar mass-to-light is a free parameter and we used a constant mass-to-light ratio (M/L_*) Sérsic model (see Romanowsky et al. 2009) that uses a galaxy's field stars and for which the circular velocity (based only on the visible, i.e. stellar matter) is:

$$v_c^2(r) \equiv \frac{GM(r)}{r}$$
$$= \frac{G(M/L_*)L_*}{r}\left\{1 - \frac{\Gamma\left[(3-p)n_*, (r/a_{\rm s}^*)^{1/n_*}\right]}{\Gamma\left[(3-p)n_*\right]}\right\}, (6)$$

where n_* and $a_{\rm s}^*$ are the Sérsic index and scale radius for the stellar component, and p is a function of n_*. For further details the reader is referred to our recent paper S14. To this visible mass we add the dark component given with the NFW model: thus, the free parameters of the NFW model are: M/L_* (*stellar* mass-to-light ratio), $\rho_{\rm s}$ and $r_{\rm s}$.

For our NFW models we calculate the concentration parameter ($c_{\rm vir} \equiv r_{\rm vir}/r_{\rm s}$) and compare the obtained values with the estimates we obtained previously in S14: for calculations, we use the virial mass, $M_{\rm vir} \equiv 4\pi\Delta_{\rm vir}\rho_{\rm crit}r_{\rm vir}^3/3$, where the critical density is $\rho_{\rm crit} = 1.37 \times 10^{-7}M_\odot{\rm pc}^{-3}$ and the critical overdensity is $\Delta_{\rm vir} = 101$.

In Fig. 3 we present three best-fitting results for tested anisotropies. It can be seen that the isotropic model better fits the outermost parts of the galaxy, whereas the tangentially anisotropic model better fits the innermost points. The theoretically based model is in between the two aforementioned models. Taking into account the uncertainties related to anisotropy, we calculated the following value of the concentration parameter of the NFW halo and the virial mass: $c_{\rm vir} = 12.96 \pm 2.27$ and $M_{\rm vir} = (1.54 \pm 0.75) \times 10^{12}M_\odot$.
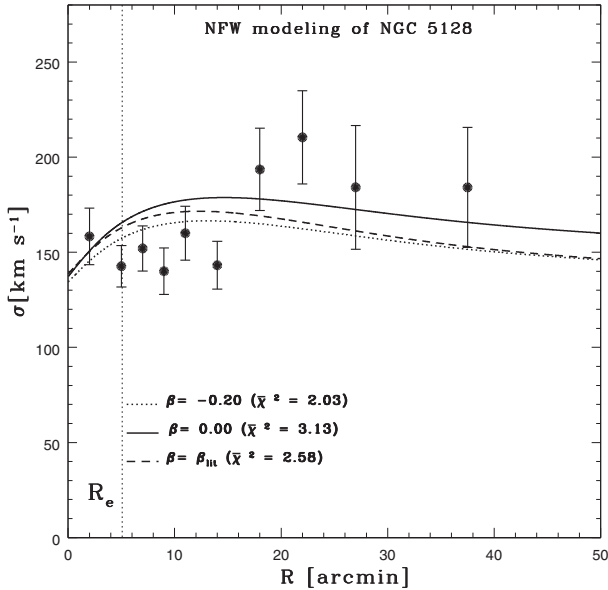
Fig. 3. *NFW modeling of the GCs of NGC 5128. The solid line is for the isotropic case ($\beta = 0$) for which mass-to-light of the stellar component in the B-band is $M/L_* = 4.0$ and $r_s = 1200$ arcsec and $\rho_s = 0.0350 M_\odot \mathrm{pc}^{-3}$. The dotted line is for the case of mildly tangential anisotropies ($\beta = -0.20$) for which $M/L_* = 3.5$ and $r_s = 1200$ arcsec and $\rho_s = 0.0300 M_\odot \mathrm{pc}^{-3}$. The dashed line is for the radially anisotropic theoretical case ($\beta = \beta_{\mathrm{lit}}$), for which $M/L_* = 4.0$ and $r_s = 1200$ arcsec and $\rho_s = 0.0450 M_\odot \mathrm{pc}^{-3}$.*

3.2. MOND models

We tested three MOND models using the Jeans equation in the spherical approximation. The methodology used in the present paper is described in detail in S14 and here we provide again some necessary basic information. It is important to stress that in all MOND models there is *only one* free parameter, the total stellar mass-to-light ratio, based only on the visible stellar mass. The value of the mass-to-light ratio which best describes the observed velocity dispersions is varied and in three plots below we present the best-fitting cases.

The Newtonian acceleration is given as $a_\mathrm{N} = a\mu(a/a_0)$, where a is the MOND acceleration, a_0 is the universal constant ($a_0 = 1.35^{+0.28}_{-0.42} \times 10^{-8}$ cm s^{-2}, Famaey et al. 2007) and $\mu(x)$ is the MOND interpolating function which is different for each MOND model. We tested three MOND models to infer whether the additional DM component is needed and whether MOND alone is sufficient to correctly describe the dynamics of NGC 5128. For some galaxies investigated so far, we have encountered mixed results: some galaxies could be fitted in MOND without the need of DM, while, on the other hand, some other objects needed an additional dark component

(see S14). The comparison of NGC 5128 with other galaxies and placing it into a wider context will be given below.

A simple MOND formula (Famaey and Binney 2005) is given by (the expression for x is given above and is valid in all MOND cases):

$$\mu(x) = \frac{x}{1+x}. \tag{7}$$

A standard MOND formula (Sanders and McGaugh 2002) is given by:

$$\mu(x) = \frac{x}{\sqrt{1+x^2}}. \tag{8}$$

The toy MOND model (Bekenstein 2004) is described with:

$$\mu(x) = \frac{-1 + \sqrt{1+4x}}{1 + \sqrt{1+4x}}. \tag{9}$$

The expressions for the circular velocities for all three functions are given in Samurović and Ćirković (2008).

We use the three MOND models because usually in the literature one finds one MOND formula applied for a given object and our goal is to provide the range of the calculated mass-to-light ratios that are as accurate as possible in order to be compared with predictions coming from the SPS models (where also various ranges are available).
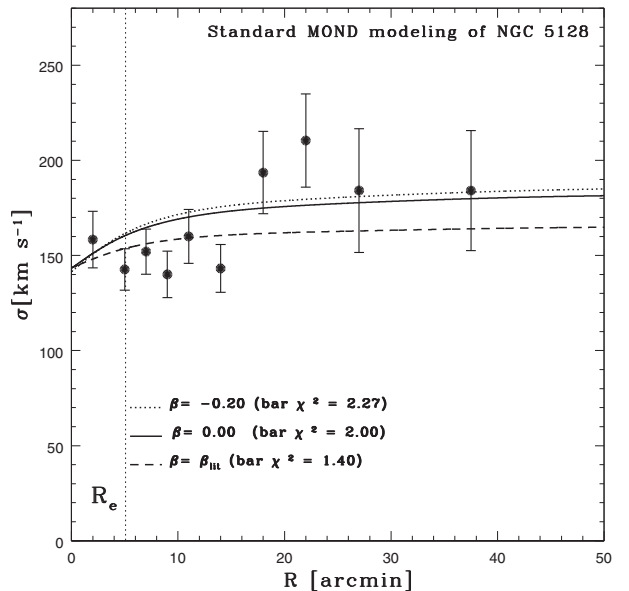
Fig. 4. *The MOND modeling of GCs of NGC 5128 for the standard formula. The meaning of the types of lines used is the same as in Fig. 2. The values of the mass-to-light ratio of the stellar component for each case are: 5.8, 5.0 and 6.0 for isotropic, tangentially anisotropic and radially anisotropic theoretical case, respectively.*

15

The standard MOND model in Fig. 4 can provide a good fit for the velocity dispersion profile of NGC 5128 without the need of DM in all three cases and the obtained values of the mass-to-light ratio are between 5.0 and 6.0 in the B-band. This value is in agreement with the best-fitting values coming from the BC and PEGASE SPS models with the Salpeter IMF (see Table 2). Both isotropic and tangentially anisotropic models provide better fits in the outermost regions whereas the radially anisotropic model provides better fit in the inner region.

The simple MOND model in Fig. 5 in all three cases of anisotropy provides good fits with similar quality and the obtained values of the mass-to-light ratio are between 3.4 and 4.8 in the B-band, in agreement with the IP13 models with the Kroupa IMF. Again, there is no need for the introduction of DM in this case.
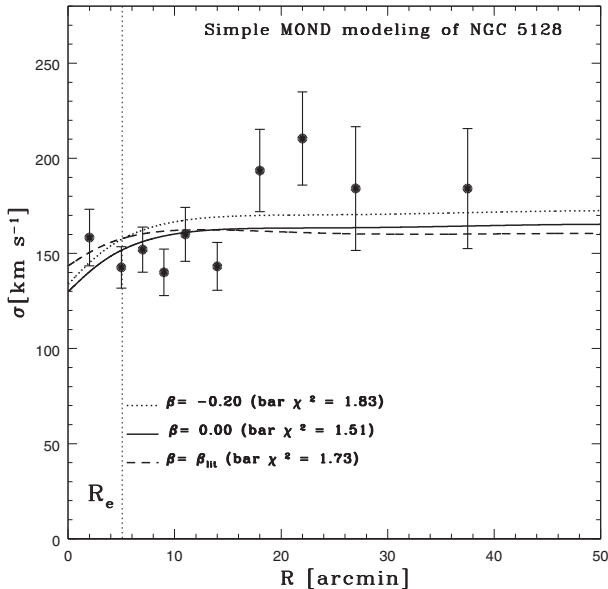

Fig. 5. *The MOND modeling of GCs of NGC 5128 for the simple formula. The meaning of the types of lines used is the same as in Fig. 2. The values of the mass-to-light ratio of the stellar component for each case are: 3.6, 3.4 and 4.8 for isotropic, tangentially anisotropic and radially anisotropic theoretical case, respectively.*

Finally, the toy MOND model in Fig. 6 also provides a good fit with the values of the mass-to-light ratios between 3.0 and 4.0 in the B-band, values again in agreement with the IP13 models with the Kroupa IMF. The isotropic and tangentially anisotropic models also provide better fits in the outermost regions, whereas the radially isotropic model provides a marginally better fit in the inner region. Since the values of the inferred mass-to-light ratio are lowest of all three tested MOND models, again there is no need for the additional DM in the mass budget of NGC 5128.
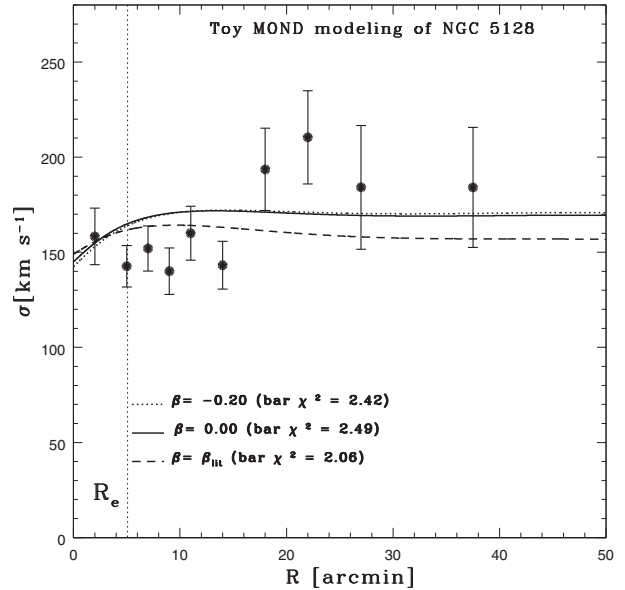
Fig. 6. *The MOND modeling of GCs of NGC 5128 for the toy formula. The meaning of the types of lines used is the same as in Fig. 2. The values of the mass-to-light ratio of the stellar component for each case are: 3.6, 3.0 and 4.0 for isotropic, tangentially anisotropic and radially anisotropic theoretical case case, respectively.*
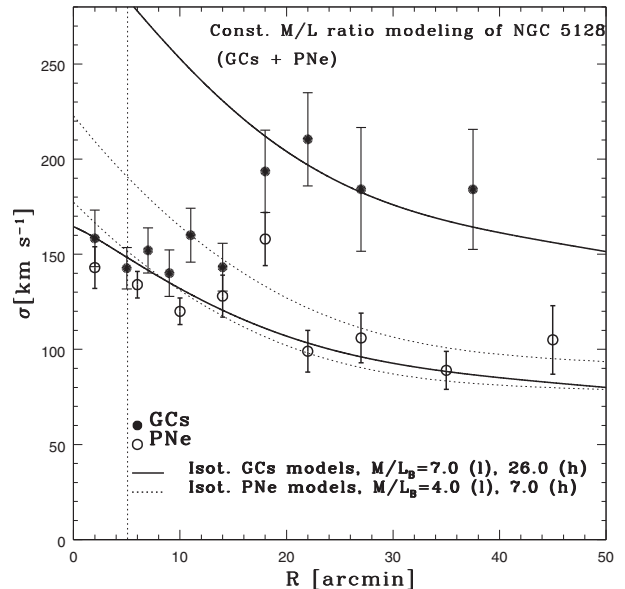
Fig. 7. *Comparison of two isotropic Jeans models based on GCs from the present paper and on PNe based on Samurović (2006). For the models based on GCs (filled circles), two isotropic models (solid lines) are taken from Fig. 2: the lower line ("l") is for $M/L_B = 7.0$ and the higher ("h") line is for $M/L_B = 26.0$. The isotropic Jeans models (dotted lines) based on PNe (open circles) are taken from Samurović (2006) and are for $M/L_B = 4.0$ (lower, "l", line) and $M/L_B = 7.0$ (higher, "h", line).*

3.3. Comparison with PNe data

In Fig. 7 we present the comparison of the isotropic Jeans models based on GCs from the present paper and the results based on PNe from Samurović (2006). It is obvious that beyond $\sim$ 20 arcmin the velocity dispersion of two different populations starts to diverge. Whereas the velocity dispersion based on GCs remains approximately constant at $\sigma \sim 200$ km s^{-1}, the values of the velocity dispersion based on PNe show again approximately constant trend but are much lower, $\sigma \sim 100$ km s^{-1}. The consequence of this is serious: whereas in the case of GCs a significant amount of DM is necessary to model the observed kinematics, in the case of PNe, the outer points can be modeled without DM, i.e. with $M/L_B = 7$ (see the upper dotted line in Fig. 7).

4. DISCUSSION

From what has been found above based on GCs as a tracer of the total dynamical mass, it is obvious that NGC 5128 is an example of the massive ETG embedded in a massive dark halo, when one works in the Newtonian approach. The DM matter begins to dominate beyond $\sim 3R_e$ and in the outermost regions it is the dark, invisible, component that dominates luminous matter. This is in agreement with the results found for other ETGs, such as NGC 4472 (Samurović 2012), NGC 1407 (S14) and NGC 5846 (S14). The Newtonian mass-follows-light light model is close to the prediction based on the Salpeter function in the inner parts, whereas NFW DM is consistent with the lower value of the stellar mass-to-light ratio (based on the Kroupa IMF) which implies approximately equal contribution of visible and DM interior to $\sim 3R_e$.

On the other hand, when one works within the MOND framework, one can see that all tested MOND models successfully fit the dynamics of NGC 5128 and that DM is not required for any of the tested models: the inferred values of the mass-to-light ratios are fully in agreement with the estimates coming from several tested SPS models. Two MOND models (simple and toy) prefer lower values of the stellar mass-to-light ratio, based on the Kroupa IMF whereas the standard MOND model is consistent with the prediction based on the Salpeter IMF (see Table 2).

The comparison of results obtained in the present paper to our previous findings leads us to note the following:

i) The sample of GCs from Samurović (2006) was much smaller and it comprised 215 clusters. The biggest difference is the number of objects per bin beyond 16 arcmin: in Samurović (2006) there were only 41 objects whereas in the present paper the number is nearly tripled since we now have 110 GCs there. This has enabled us to better determine the values of the velocity dispersion in the outer regions of

NGC 5128: in the previous paper the velocity dispersion was ≈ 150 km s^{-1} whereas with the additional GCs, we now calculate higher values, i.e. $\sigma \approx 190$ km s^{-1}.

ii) In Samurović (2010) we used a sample of 780 PNe whose profile of velocity dispersion has a declining trend which enabled us to model the dynamics of NGC 5128 without DM. The outermost point at $\sim$ 60 arcsec was discrepant and implied a rise of the total mass indicative of DM, or strong tangential anisotropies. The future studies with more tracers should clarify the discrepancy present at this stage. Similar discrepancy related to the inferred mass based on different tracers is also present in the case of ETG NGC 821: the total cumulative mass inferred from GCs is higher than that calculated using PNe (S14).
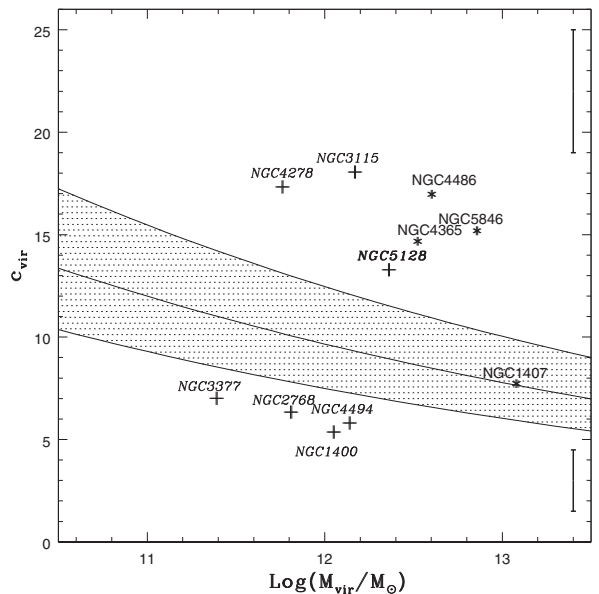
Fig. 8. *The concentration parameter as a function of virial mass (expressed in solar units). NGC 5128, the subject of the present paper, is plotted using bold characters, whereas other galaxies from S14 are plotted using normal characters: the names of the slow (fast) rotators are plotted using roman font characters with "∗" sign (italics with "+" sign) The central line of the hatched region is given by Eq. 10 and its limits are determined with 1σ scatter. The vertical solid lines on the right hand side of the plot represent the typical error bars for the concentration parameter for two classes of galaxies: the lower line is for the objects below the hatched region and the higher line is for the objects above the hatched region.*

We now want to place NGC 5128 within the context of other ETGs and the results of numerical simulations: in Fig. 8 we show the dependence of the concentration parameter as a function of the virial mass. The shaded area represents the region determined by the mean relation expected from ΛCDM (cold dark matter plus cosmological constant) model for which the central line is given with:

17

$$c_{\text{vir}}(M_{\text{vir}}) \simeq 12 \left(\frac{M_{\text{vir}}}{10^{11} M_{\odot}} \right)^{-0.094}, \qquad (10)$$

and the limits are determined with 1σ scatter (equal to 0.11 dex, see for example, Napolitano et al. 2011). The ten galaxies come from S14 (see Fig. 24 therein) and are divided into two classes, slow and fast rotators. NGC 5128 is a fast rotator (Coccato et al. 2009) and obviously has the largest virial mass within its class. Although situated slightly above the region predicted by ΛCDM simulations, it is marginally consistent with the model, given the calculated error bars. Interestingly, NGC 5128 is the only galaxy in the group of objects above the hatched region which does not need additional DM in the MOND approach.

5. CONCLUSIONS

In this paper we investigated the kinematics calculated from observations of GCs by Woodley et al. (2010) in the ETG NGC 5128 and analyzed its dynamics using both the Newtonian and MOND methodologies for three values of anisotropy (isotropic orbits, tangentially dominated orbits, and radially dominated orbits). From the available observational data we calculated velocity dispersions and skewness and kurtosis parameters using standard statistical procedures. We used the Jeans equation to make dynamical models of NGC 5128 for the purpose of establishing the importance of DM in this object.

Our conclusions are as follows.

(1) We found that the departures from the Gaussian (given with the skewness and kurtosis parameters, s_3 and s_4, estimated from the radial velocities of the saple of GCs) are not large and, in most of the bins, consistent with isotropic distribution. There are two regions with different values of the velocity dispersion: in the inner region (interior up to $\sim 3R_{\text{e}}$) the value of velocity dispersion is approximately 150 km s^{-1} whereas beyond $\sim 3R_{\text{e}}$ it rises to approximately 190 km s^{-1}, implying the increase of the DM contribution there.

(2) We showed that Newtonian mass-follows-light cannot provide a successful fit the velocity dispersion for the whole galaxy and that the additional, dark component, is necessary since the mass-to-light ratio in the inner region, $M/L_B \sim 7.0$, rises to $M/L_B \sim 26.0$ in the outer regions beyond 3 effective radii. We tested the NFW model with DM and found that it can provide a good fit to the dynamics of NGC 5128.

(3) We tested three MOND models (standard, simple and toy) and found that they all provide good fits to the observed velocity dispersion without the need of DM.

(4) We used the predictions of several SPS models and found that NFW model and simple and toy MOND models agree with the results based on the Kroupa IMF. The Newtonian mass-follows-light model which provides a good fit in the inner region of NGC 5128 and the standard MOND model are based on the Salpeter IMF.

(5) The position of NGC 5128 on the $M_{\text{vir}} - c_{\text{vir}}$ plot is slightly above the region predicted by numerical simulations performed in the framework of the ΛCDM cosmology. We found that NGC 5128 has the largest value of the calculated virial mass of fast rotators ETGs that we studied to date and is the only galaxy above the predicted region for which DM is not needed in the MOND approach.

(6) When we compare the results obtained using GCs with other tracers, we can reach the ambiguous conclusions: on the one hand, the results based on GCs are in agreement with studies based on the rotation curve of NGC 5128 based on neutral hydrogen, because van Gorkom et al. (1990) found a flat rotation curve and measured its maximum velocity of 265 km s^{-1} which implies the existence of DM, and on the other hand, the modeling results based on the velocity dispersion profile obtained using PNe (Samurović 2006) suggest the lack of DM in the outer parts of NGC 5128. This interesting discrepancy strongly suggests that further observations using various tracers of the mass of the well-known ETG NGC 5128 are still necessary and that the usage of new improved dynamical models will hopefully resolve the present ambiguity.

REFERENCES

Angus, G. W., Diaferio, A., Famaey, B. and van der Heyden, K. J.: 2013, *Mon. Not. R. Astron. Soc.*, **436**, 202.
Bekenstein, J.: 2004, *Phys. Rev. D*, **70**, 083509.
Bertin, G.: 2014, Dynamics of Galaxies, Second Edition, Cambridge Univ. Press, Cambridge.
Bell, E.F. and de Jong, R.S., 2001, *Astrophys. J.*, **550**, 212.
Bílek, M., Jungwiert, B., Ebrová, I. and Bartošková, K. 2015, *Astron. Astrophys.*, **575**, A29.
Binney, J. J. and Tremaine, S.: 2008, Galactic Dynamics, Second Edition, Princeton Univ. Press, Princeton.
Binney J. J. and Merrifield M. R.: 1998, Galactic Astronomy, Princeton Univ. Press, Princeton.
Binney J. J. and Mamon, G.: 1982, *Mon. Not. R. Astron. Soc.*, **200**, 361.
Bradač, M., Clowe, D., Gonzalez, A. H., et al.: 2006, *Astrophys. J.*, **652**, 937.

Bruzual, G. and Charlot, S.: 2003, *Mon. Not. R. Astron. Soc.*, **344**, 1000.

Coccato, L., Gerhard, O., Arnaboldi, M., Das, P., Douglas, N. G., Kuijken, K., Merrifield, M. R., Napolitano, N. R., Noordermeer, E., Romanowsky, A. J., Capaccioli, M., Cortesi, A., de Lorenzi, F. and Freeman, K. C.: 2009, *Mon. Not. R. Astron. Soc.*, 394, 1249.

Deason, A. J., Belokurov, V., Evans, N. W. and McCarthy, I. G.: 2012, *Astrophys. J.*, **748**, 2.

de Lorenzi, F., Gerhard, O., Coccato, L., Arnaboldi, M., Capaccioli, M., Douglas, N. G., Freeman, K. C., Kuijken, K., Merrifield, M. R., Napolitano, N. R., Noordermeer, E., Romanowsky, A. J. and Debattista, V. P.: 2009, *Mon. Not. R. Astron. Soc.*, **395**, 76.

Dufour, R. J., Harvel, C. A., Martins, D. M., Schiffer, F. H. III, Talent, D. L., Wells, D. C., van den Bergh, S. and Talbot, R. J. Jr.: 1979, *Astron. J.*, **84**, 284.

Duncan, M.J. and Wheeler, J.C.: 1980, *Astrophys. J.*, **237**, L27.

Famaey, B. and Binney, J.: 2005, *Mon. Not. R. Astron. Soc.*, **363**, 603.

Famaey, B., Bruneton, J.-P. and Zhao, H.S.: 2007, *Mon. Not. R. Astron. Soc.*, **377**, L79.

Fioc, M. and Rocca-Volmerange, B.: 1997, *Astron. Astrophys.*, **326**, 550.

Foster, C., Pastorello, N., Roediger, J., Brodie, J. P, Forbes, D. A., Kartha, S. S., Pota, V., Romanowsky, A. J., Spitler, L. R., Strader, J., Usher, C. and Arnold, J. A.: 2015, *Mon. Not. R. Astron. Soc.*, accepted (arXiv:1512.06130v1).

Gerhard, O.: 1993, *Mon. Not. R. Astron. Soc.*, **265**, 213.

Into, T. and Portinari, L.: 2013, *Mon. Not. R. Astron. Soc.*, **430**, 2715.

Israel, F. P.: 1998, *Astron. Astrophys. Rev.*, **8**, 237.

Jeans, J. H.: 1915, *Mon. Not. R. Astron. Soc.*, **76**, 70.

Kleinheinrich, M., Schneider, P., Rix, H.-W., Erben, T., Wolf, C., Schirmer, M., Meisenheimer, K., Borch, A., Dye, S., Kovacs, Z. and Wisotzki, L.: 2006, *Astron. Astrophys.*, **455**, 441.

Mamon, G. A. and Łokas, E. L.: 2005, *Mon. Not. R. Astron. Soc.*, **362**, 95.

Napolitano, N. R., Romanowsky, A. J., Capaccioli, M., Douglas, N. G., Arnaboldi, M., Coccato, L., Gerhard, O., Kuijken, K., Merrifield, M. R., Bamford, S. P., Cortesi, A., Das, P. and Freeman, K. C.: 2011, *Mon. Not. R. Astron. Soc.*, **411**, 2035.

Navarro, J. F., Frenk, C. S. and White, S. D. M.: 1997, *Astrophys. J.*, **490**, 493.

Pota, V., Forbes, D. A. Romanowsky, A. J., Brodie, J. P., Spitler, L. R., Strader, J., Foster, C., Arnold, J. A., Benson, A., Blom, C., Hargis, J. R., Rhode, K. L. and Usher, C.: 2013, *Mon. Not. R. Astron. Soc.*, **428**, 389.

Rejkuba, M.: 2004, *Astron. Astrophys.*, **413**, 903.

Romanowsky, A. J., Douglas, N.G., Arnaboldi, M., Kuijken, K., Merrifield, M. R., Napolitano, N. R., Capaccioli, M. and Freeman, K. C.: 2003, *Science*, **5640**, 1696.

Romanowsky A. J., Strader J., Spitler L. R., Johnson R., Brodie J. P., Forbes D. A. and Ponman T.: 2009, *Astron. J.*, 137, 4956.

Samurović, S.: 2006, *Serb. Astron. J.*, **173**, 35.

Samurović S.: 2007, *Publ. Astron. Obs. Belgrade*, **81**, 1.

Samurović, S.: 2010, *Astron. Astrophys.*, **514**, A95.

Samurović, S.: 2012, *Astron. Astrophys.*, **541**, A138.

Samurović, S.: 2014, *Astron. Astrophys.*, **570**, A132 (S14).

Samurović, S. and Danziger, I. J.: 2005, *Mon. Not. R. Astron. Soc.*, **363**, 769.

Samurović, S. and Ćirković M. M.: 2008, *Astron. Astrophys.*, **488**, 873.

Samurović, S., Vudragović, A., Jovanović, M. and Ćirković M. M.: 2014, *Serb. Astron. J.*, **188**, 29.

Sanders, R. H. and McGaugh, S.: 2002, *Ann. Rev. Astron. & Astrophys.*, **40**, 263.

Tonry, J. L.: 1983, *Astrophys. J.*, **266**, 58.

Tortora, C., Napolitano, N. R., Romanowsky, A. J. and Jetzer, P.: 2010, *Astrophys. J.*, 721, L1.

van Gorkom, J. H., van der Hulst, J. M., Haschick, A. D. and Tubbs, A. D.: 1990, *Astron. J.*, 99, 1781.

Woodley, K. A., Gómez, M, Harris, W. E., Geisler, D. and Harris, G. L. H.: 2010, *Astron. J.*, **139**, 1871.

ЊУТНОВСКИ И MOND ДИНАМИЧКИ МОДЕЛИ ГАЛАКСИЈЕ NGC 5128: ПРОУЧАВАЊЕ ДОПРИНОСА ТАМНЕ МАТЕРИЈЕ

S. Samurović

Astronomical Observatory, Volgina 7, 11060 Belgrade 74, Serbia

E–mail: *srdjan@aob.rs*

У раду је анализирана позната блиска галаксија раног типа NGC 5128 (Centaurus A) и коришћен је узорак њених глобуларних јата у циљу анализе динамике ове галаксије. Проучаван је њутновски приступ као и MOND модел и то користећи три вредности за анизотропију кретања јата у галаксији. Проучавани су изотропни случај, благо тангенцијални случај као и радијално анизотропни случај заснован на доступној литератури. Пронађено је да у оквиру ове галаксије постоје две области са различитим вредностима дисперзије брзина: у области унутар три ефективна радијуса њена вредност је око 150 km s^{-1}, док се изван три ефективна радијуса вредност дисперзије брзина повећава и износи око 190 km s^{-1}, што имплицира повећање укупне кумулативне масе што је индикативно за постојање тамне материје у тим областима, у оквиру њутновског приступа: однос маса-сјај се повећава са $M/L_B = 7$ у унутрашњим на $M/L_B = 26$ у спољним областима. Пронађено је да Наваро-Френк-Вајтов модел са тамним халоом добро описује динамику галаксије NGC 5128. Користећи три MOND модела (стандардни, једноставни и "модел-играчку") пронађено да сви они добро фитују дисперзију брзина галаксије NGC 5128 и да у оквиру модела MOND није потребна додатна, тамна компонента.